

## A “ladder” Morphology in an ABC Triblock Copolymer

Takeshi Kaneko,<sup>1</sup> Kazuya Suda,<sup>1</sup> Kotaro Satoh,<sup>2</sup> Masami Kamigaito,<sup>2</sup>  
Toshinori Kato,<sup>3</sup> Tomohiro Ono,<sup>3</sup> Eiji Nakamura,<sup>3</sup> Toshio Nishi,<sup>4</sup> Hiroshi Jinnai<sup>\*1</sup>

**Summary:** ABC triblock copolymers are known to exhibit a wide variety of unique types of morphologies compared to AB diblock copolymers. In the present study, poly(styrene-block-(ethylene-alt-propylene)-block-(methyl methacrylate)) (SEPM) triblock copolymers were synthesized and their morphologies were extensively studied by transmission electron microtomography (TEM). In the SEPM triblock copolymer, two kinds of morphologies coexist: One was the well-known knitting morphology, and the other was a novel morphology called the “ladder morphology”. The ladder morphology was a major morphology in the SEPM copolymer, the stability of which was discussed in terms of the interfacial area and the solubility parameters between the three components.

**Keywords:** Block copolymers; Electron tomography; Nanostructure; TEM; Three-dimensional reconstruction

### Introduction

Block copolymers exhibit various periodic microphase-separated structures due to the immiscibility between the dissimilar sequences.<sup>1–7</sup> In case of the classical two-component linear block copolymers, the nanoscale structures include spheres of A(B) on a body-centered cubic lattice in a B(A) matrix, cylinders of A(B) on a hexagonal lattice in a B(A) matrix, and coalternating lamellae. Besides these rather simple morphologies, several complex (bicontinuous) nanostructures – the perforated lamellar, gyroid, and double-diamond morphologies were reported.<sup>5–7</sup> Of considerable recent interest is the much larger variety of nano-

scale structures of more complex classes of block copolymers than the simple linear diblock copolymers. For example, Stadler *et al.* observed a series of intriguing morphologies in the ABC-type linear triblock copolymers.<sup>8–10</sup> In particular, the “knitting morphology” observed in a poly(styrene-block-(ethylene-co-butylene)-block-(methyl methacrylate)) (SEBM) is a fascinating one.<sup>9</sup> Mogi *et al.* found an “ordered tricontinuous double-diamond (OTDD)” morphology of a poly(isoprene-block-styrene-block-2-vinylpyridine) (ISP), in which two non-intersecting channels consisting of either I or P domains with  $F\bar{4}3m$  symmetry were observed.<sup>11</sup> Other interesting morphologies such as the “helical morphology”, and “spheres on cylinder morphology” were also found.<sup>10,12</sup> Rearranging the molecular architecture from linear to star or brush may make the variety of microphase-separated structures even wider.<sup>13–19</sup>

Although some extensive work has been carried out with the aim of understanding the morphological behavior of the ternary ABC triblock copolymers as a function of their relative composition of the different components and also of the various block sequences, until now, little is known about controlling the morphologies. This is be-

<sup>1</sup> Department of Macromolecular Science and Engineering, Kyoto Institute of Technology, Matsugasaki, Kyoto 606-8585, Japan  
Fax: +81-75-724-7770  
E-mail: hjinnai@kit.ac.jp

<sup>2</sup> Department of Applied Chemistry, Nagoya University, Furo-cho, Chikusa-ku, Nagoya 464-8603, Japan

<sup>3</sup> Kuraray Co. Ltd., 2045-1, Sakazu, Kurashiki, Okayama 710-8691, Japan

<sup>4</sup> Department of Organic and Polymeric Materials, School of Science and Engineering, Tokyo Institute of Technology, 2-12-1, Ohokayama, Meguro-ku, Tokyo 152-8552, Japan

cause the self-assembled nanostructures are often too complicated to be evaluated by conventional experimental techniques, e.g., transmission electron microscopy (TEM) or X-ray (neutron) scattering. In the present study, transmission electron microtomography (TEMT), which enables us to observe nano-scale morphologies in three-dimension (3D), is utilized to investigate the microphase-separated structures of the poly(styrene-block-(ethylene-alt-propylene)-block-(methyl methacrylate)) (SEPM) triblock copolymers. A new morphology, which we called the “ladder morphology”, similar to the “knitting morphology” was found. The stability of the ladder morphology was discussed in terms of the segmental interactions between the three components and interfacial areas per unit volume.

## Experimental

### Materials

Poly(styrene-block-isoprene-block-methyl methacrylate) (SIM) triblock copolymers were prepared via sequential living anionic polymerization according to the literature.<sup>20</sup> Furthermore, the central polyisoprene block of SIM was hydrogenated to afford the corresponding poly(styrene-block-(ethylene-alt-propylene)-block-(methyl methacrylate)) (SEPM) triblock copolymers. Some samples were fractionated by preparative GPC (column: Shodex K-2003) in CHCl<sub>3</sub> to obtain polymers with narrower molecular weight distributions ( $M_w/M_n < 1.1$ ). Based on <sup>1</sup>H NMR spectroscopy, the volume fractions of the PS and PEP in the SEPM copolymer were determined to be 0.35 and 0.32, respectively. The number average molecular weight ( $M_n$ ) of the triblock copolymer was 83,900 against polystyrene standard samples, and thus those of each PS, PEP, and PMMA block were estimated to be 29,300, 23,500, and 31,100, respectively.

### Specimens

A film specimen was prepared by casting from an ca. 5wt% chloroform solution. The

cast film was annealed at 175 for 48 hours under vacuum. The film was stained by contact with ruthenium tetroxide (RuO<sub>4</sub>) vapor for 2 minutes or iodine (I<sub>2</sub>) vapor for 24 hours. The ultra-thin sections were prepared by microtoming (Reichert-Jung Ultracut-S) using a diamond knife (DiATOME cryo dry) at cryogenic temperature ( $\sim -120^\circ\text{C}$ ). A ultrathin section of ca. 100 nm thick was transferred onto a Cu mesh grid with a polyvinylformal substrate. Prior to the TEMT observations, 5 nm Au nanoparticles were deposited from an aqueous suspension (GCN005, BBL International Ltd., UK).

### Transmission Electron Microtomography

TEMT experiments were performed by energy-filtering transmission electron microscopy with a field-emission gun operated at 200 kV (JEM-2200FS, JEOL Co., Ltd., Japan). Projections were collected using a slow-scan CCD camera (Gatan USC1000, Gatan, Inc., USA). Note that only the transmitted and elastically scattered electrons (electron energy loss of  $0 \pm 15$  eV) were selected by an in-column energy filter installed in the JEM-2200FS (Omega filter, JEOL, Ltd., Japan) in order to obtain achromatic projections. The series of TEM micrographs of the ladder morphology were taken over the tilt angle from  $-70^\circ \sim 64^\circ$  at  $1^\circ$  increments. On the other hand, the series of TEM micrographs of the knitting morphology were taken over the tilt angle from  $-60^\circ \sim 60^\circ$  at  $1^\circ$  increments. The pixel size was ca. 1 nm. A projection at each tilt angle was acquired with the frame size of 1024 by 1024 pixels. Subsequently, the tilt series of the TEM micrographs were aligned by the fiducial marker method<sup>21</sup> with the Au nanoparticles as the fiducial markers and then reconstructed on the basis of the filtered-back-projection (FBP) method.<sup>22,23</sup> All reconstruction procedures were carried out using software developed in our laboratory.

## Results and Discussion

Figure 1 shows TEM micrograph of SEPM triblock copolymer. The grey part of the

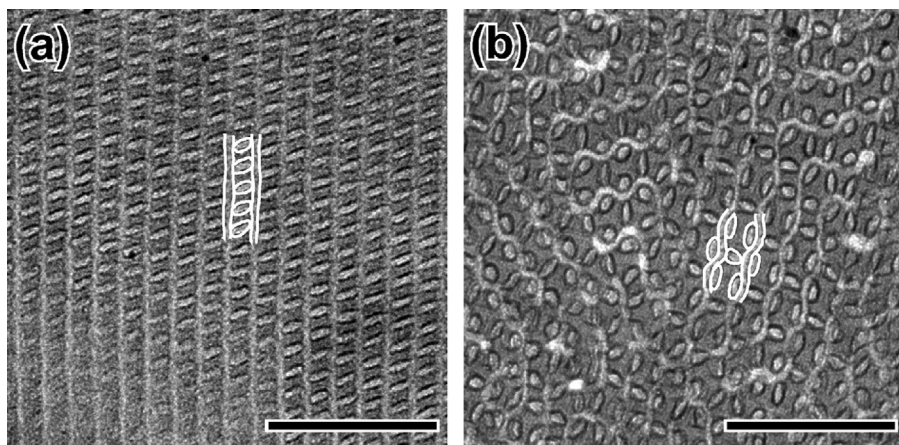


**Figure 1.**

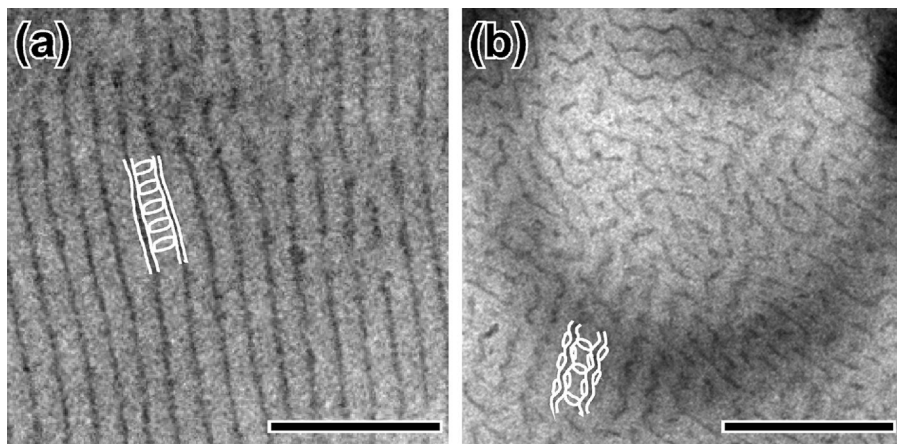
TEM micrographs of (a) ladder and (b) knitting morphologies of SEPM triblock copolymer stained by  $\text{RuO}_4$ . Gray domains are PS microdomains. Ladder and knitting morphologies are schematically drawn. Bar represents 200 nm.

figure corresponds to the  $\text{RuO}_4$ -stained PS microdomain. Two kinds of microphase-separated structures were observed: The major one is a “ladder morphology” that consists of lines and ellipsoidal domains. The morphological features of the ladder morphology are illustrated in Figure 1(a). In another field of view, the minor morphology, the knitting morphology, was also observed [see Figure 1(b)]. As schematically illustrated in Figure 1(b), the knitting morphology is made of wavy lines and ellipsoidal domains. In contrast to the ladder morphology, 2/3 of the ellipsoidal microdomains in the unit cell are aligned parallel to the wavy microdomains, while the remaining 1/3 was perpendicular to them, which is exactly the same morphology as reported by Breiner *et al.* in 1996.<sup>9</sup>

Since the lines and ellipsoids appeared to be white in Figure 1, they are either PMMA or PEP domains. In order to distinguish one from the other, the SEPM was stained by iodine as shown in Figure 2. The dark part of the figure now corresponds to the  $\text{I}_2$ -stained PMMA microdomain. Figures 2(a) and 2(b) correspond, respectively, to the ladder and knitting morphologies. The microphase-separated structures evaluated from the  $\text{RuO}_4$ -stained section are schematically shown in the figure. The linear (or wavy) micro-

domains were found to be stained by the iodine, meaning that they are PMMA domains. Therefore, the ellipsoidal microdomains are assigned to the PEP microdomains. Note here that the knitting morphology in our SEPM is essentially the same structure as that already reported except for the fact that the wavy domain was the PEP domain instead of the PEB domain in Breiner’s SEBM.<sup>9</sup>

Now that the three microdomains were assigned, TEMT observations were carried out for the two morphologies. Figure 4 shows the 3D reconstructed images of the ladder and knitting morphologies. From the 3D reconstructed images, it became obvious that both the ladder and knitting morphologies had cylinder-like two-dimensional morphologies. The 3D model proposed for the knitting morphology in the literature<sup>9</sup> is proven to be correct based on our TEMT result [Figure 4(b)]. A volumetric analysis of the reconstruction (of both the ladder and knitting morphologies) yields the volume fractions of the three components,  $f_{\text{PS}}=0.36$ ,  $f_{\text{PEP}}=0.32$  and  $f_{\text{PMMA}}=0.32$ , that are in excellent agreement with the known composition of the copolymer ( $f_{\text{PS}}=0.35$ ,  $f_{\text{PEP}}=0.32$  and  $f_{\text{PMMA}}=0.33$ ). Note that the volume fractions did not depend on the type of morphology.



**Figure 2.**

TEM micrographs of (a) ladder and (b) knitting morphologies of SEPM triblock copolymer stained by iodine. Gray domains correspond to PMMA microdomains. Schematic in (a) and (b) show ladder and knitting morphologies, respectively. Bar represents 200 nm.

The possible chain packing inside the SEPM microdomains is schematically shown in Figure 3. The interfaces between the three microdomains are shown by the solid line on which the PS-PEP and PEP-PMMA chemical junctions are placed. It is intriguing that there was an interface where no chemical junction exists, i.e., the interface between the PS and PMMA microdomains. In the microphase-separated structures of the diblock copolymers, such an interface will not

be found. When comparing the ladder and knitting morphologies, chain packing seems to be less frustrated for the knitting morphology than for the ladder morphology due to the following reasons: The ellipsoidal PEP microdomains whose long axis lies parallel to the PMMA wavy microdomains have a rather uniform distribution of the chemical junctions along the interface [see Figure 3(b)]. In contrast, in the ladder morphology, all of the PEP microdomains

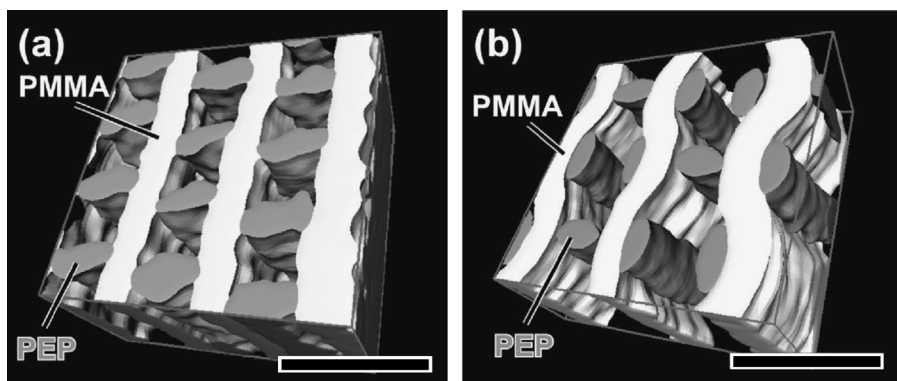


**Figure 3.**

3D reconstructed images of (a) ladder and (b) knitting morphologies. PEP and PMMA microdomains are shown by light gray and white domains, respectively. PS microdomains is left transparent. Bar represents 50 nm.

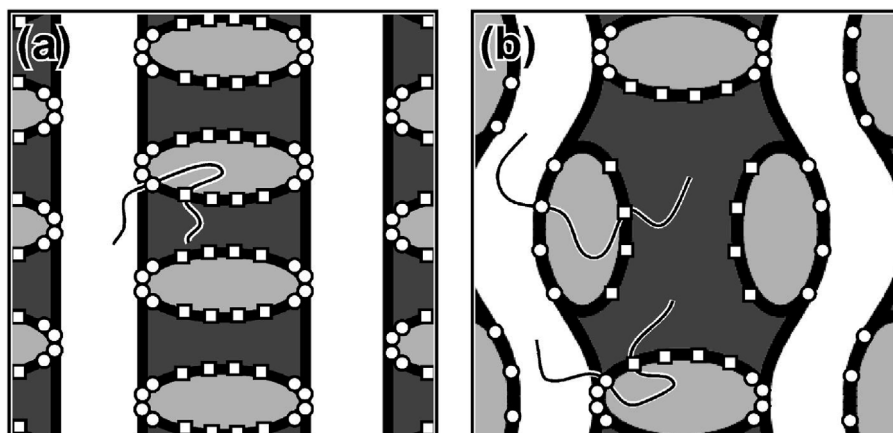


**Figure 4.**

Schematic representations of chain packing in (a) ladder and (b) knitting morphologies. PS, PEP and PMMA microdomains are shown by dark gray, light gray and white domains, respectively. PEP-PMMA and PS-PEP chemical junctions are indicated by open circles and open squares, respectively.

align their long axis perpendicular to the linear PMMA domains. In this case, the PEP-PMMA chemical junctions have to be placed as near as possible to the PEP-PMMA interface, leading to the junctions being overcrowded especially at the apex of the ellipsoid. This should increase the packing frustration of the blocks. Thus, from an entropic point of view, the ladder morphology may be less favorable than the knitting morphology, which was not the case in our TEM and TEMT experiments.

In order to provide a quantitative discussion, the interfacial area per unit volume,  $\Sigma_j$  ( $j$ : PS-PEP, PEP-PMMA and PS-PMMA), was also measured from the binarized 3D reconstructions, which are listed in Table 1.  $\Sigma_{PS-PEP}$  of the two morphologies were almost identical, while  $\Sigma_{PEP-PMMA}$  and  $\Sigma_{PS-PMMA}$  of the ladder morphology were smaller and larger than those of the knitting morphology, respectively.

Since  $\Sigma$  is affected not only by the chain conformation, but also by the (repulsive) interaction between the components, a segmental interaction parameter between the three components of the SEPM triblock copolymer is considered. The segmental interaction parameter,  $\chi$ , was calculated from the solubility parameters based on the assumption that the molar segmental volumes are given by the geometric mean of the molar volumes of the components  $i$  and  $j$ ,<sup>24</sup>

$$\chi_{ij} = (a^3/kT)(\delta_i - \delta_j)^2.$$

Where  $a$  and  $k$  are the segmental volume and the Boltzmann constant, respectively. The solubility parameters used in the calculation were 9.1, 7.9 and 9.3 for PS, PEP and PMMA, respectively [in unit of  $(\text{cal}/\text{cm}^3)^{1/2}$ ]. Table 2 lists three  $\chi$  values in the SEPM copolymer. Comparing  $\chi$  in Table 2, it became obvious that the strongest

**Table 1.**  
Interfacial area par volume for ladder and knitting morphologies

	$\Sigma_{PS-PEP}$	$\Sigma_{PEP-PMMA}$	$\Sigma_{PS-PMMA}$
Ladder morphology ( $\text{nm}^{-1}$ )	$4.0 \times 10^{-2}$	$3.0 \times 10^{-2}$	$4.7 \times 10^{-2}$
Knitting morphology ( $\text{nm}^{-1}$ )	$4.1 \times 10^{-2}$	$3.4 \times 10^{-2}$	$2.7 \times 10^{-2}$



**Table 2.**

Estimated interaction parameter ( $\chi$ ) in the SEPM triblock copolymer

	$\chi_{PS-PEP}$	$\chi_{PEP-PMMA}$	$\chi_{PS-PMMA}$
$\chi$	0.28	0.33	0.0044

incompatibility occurs between PEP and PMMA. Interestingly,  $\chi_{PS-PMMA}$  turned out to be significantly smaller than the other two interaction parameters. Therefore, from an enthalpic view point, reduction of the PEP-PMMA interfacial area is crucial; when considering the interaction parameters, creating the PS-PMMA interface does not cost much compared to creating either the PEP-PMMA or PS-PEP interfaces. Therefore, we speculate that the blocks of the SEPM copolymer had to rearrange to decrease the enthalpy at the sacrifice of their comfortable chain conformation in order to reduce the total free energy of the system. In addition, the PEP microdomains inside the PS matrix attempted to achieve a minimum interfacial area. Consequently, they formed the ellipsoidal shape with a perpendicular configuration. Hence, in the SEPM copolymer, the ladder morphology was selected due to its smaller interfacial area,  $\Sigma_{PEP-PMMA}$ , compared to the knitting morphology. In other words, the microphase-separated structure of our SEPM copolymer was an enthalpy-driven (rather than entropy-driven) structure.

Finally, we would like to make a brief comment about the knitting morphology observed in the SEBM triblock copolymer.<sup>9</sup> In this system, the author did not find the ladder morphology; only the knitting morphology was observed.<sup>9</sup> The interaction parameters,  $\chi_{PS-PEB}$  and  $\chi_{PEB-PMMA}$ , are estimated (in exactly the same way as above) to be 0.11 and 0.15, respectively. They are lower than the corresponding interaction parameters in the SEPM copolymer, meaning that the reduction of the PEB-PMMA interface is “milder” than that of the SEPM copolymer. Hence, the entropically favorable knitting morphology may be selected.

## Summary

The microphase-separated morphology of a linear ABC-type triblock copolymer, poly(styrene-block-(ethylene-alt-propylene)-block-(methyl methacrylate)) (SEPM), has been studied by transmission electron microtomography (TEMT). Two kinds of morphologies, one is a knitting morphology and the other is a new morphology called the “ladder” morphology, were found. The knitting morphology was observed in three-dimensions (3D) and found to be the same morphology already proposed by Breiner *et al.* in 1996. The interfacial areas per unit volume,  $\Sigma$ , for the three interfaces were evaluated from the 3D reconstructed images of both morphologies.  $\Sigma$  was used together with the segmental interaction parameters between the components to discuss the stability of the morphologies. It was found that the enthalpy plays a more important role than the entropy in the SEPM due to the strong incompatibility between the PEP and PMMA.

- [1] I.W. Hamley, *Nanotechnology* **2003**, 14, R39.
- [2] R. J. Spontak, M. C. Williams, and D. A. Agard. *Polymer* **1988**, 29, 387.
- [3] H. Jinnai, Y. Nishikawa, R. J. Spontak, S. D. Smith, D. A. Agard, and T. Hashimoto. *Phys. Rev. Lett.* **2000**, 84, 518.
- [4] E. L. Thomas, D. M. Anderson, C. S. Henkee, and D. Hoffman. *Nature* **1988**, 334, 598.
- [5] H. Jinnai, Y. Nishikawa, T. Ikehara, and T. Nishi. *Adv. in Polym. Sci.* **2004**, 170, 115.
- [6] A. K. Khandpur, S. Foerster, F. S. Bates, I. W. Hamely, A. J. Ryan, W. Bras, K. Almdal, and K. Mortensen. *Macromolecules* **1995**, 28, 8796.
- [7] H. Hasegawa, H. Tanaka, K. Yamasaki, and T. Hashimoto. *Macromolecules* **1987**, 20, 1651.
- [8] R. Stadler, C. Auschra, J. Beckmann, U. Krappe, I. Voigt-Martin, and L. Leibler. *Macromolecules* **1995**, 28, 3080.
- [9] U. Breiner, U. Krappe, and R. Stadler. *Macromol. Rapid Commun.* **1996**, 17, 567.
- [10] U. Krappe, R. Stader, and I. Voigt-Martin. *Macromolecules* **1995**, 28, 4558.
- [11] Y. Mogi, K. Mori, Y. Matsushita, and I. Noda. *Macromolecules* **1992**, 25, 5412.
- [12] U. Breiner, U. Krappe, V. Abetz, and R. Stadler. *Macromol. Chem. Phys.* **1997**, 198, 1051.
- [13] H. Iatrou and N. Hadjichristidis. *Macromolecules* **1992**, 25, 4649.

- [14] T. Fujimoto, H. Zhang, T. Kazama, Y. Isono, H. Hasegawa, and T. Hashimoto. *Polymer* **1992**, 33, 2208.
- [15] S. Sioula, Y. Tselikas, and N. Hadjichristidis. *Macromolecules* **1997**, 30, 1518.
- [16] V. Bellas, H. Iatrou, and N. Hadjichristidis. *Macromolecules* **2000**, 33, 6993.
- [17] H. Hiickstadt, V. Abetz, and R. Stadler. *Macromol. Rapid Commun.* **1996**, 17, 599.
- [18] A. Takano, S. Wada, S. Sato, T. Araki, K. Hirahara, T. Kazama, S. Kawahara, Y. Isono, A. Ohno, N. Tanaka, and Y. Matsushita. *Macromolecules* **2004**, 37, 9941.
- [19] K. Yamauchi, K. Takahashi, H. Iatrou, H. Hadjichristidis, T. Kaneko, Y. Nishikawa, H. Jinnai, T. Matui, H. Nishioka, M. Shimizu, and H. Furukawa. *Macromolecules* **2003**, 36, 6962.
- [20] S. Ndoni, C. M. Papadakis, F. S. Bates, and K. Almdal. *Rev. Set Instrum.* **1995**, 66, 1090.
- [21] M. C. Lawrence. "Least-squares method of alignment using markers". In J. Frank, editor, *Three-dimensional Imaging with the Transmission Electron Microscope*, Plenum Press, New York, London **1992**, p. 197.
- [22] R. A. Crowther, D. J. DeRosier, and A. Klug. *Proc. R. Soc. London* **1970**, A 317, 319.
- [23] P. F. C. Gilbert. *Proc. R. Soc. London* **1972**, B 182, 89.
- [24] L. Kane and R. J. Spontak. *Macromolecules* **1994**, 27, 663.